

CFD MODEL DEVELOPMENT FOR SUGAR MILL EVAPORATORS

Steven N. PENNISI^{1,2}, Jong-Leng LIOW² and Philip A. SCHNEIDER²

¹Sugar Research Institute, Nebo Road, Mackay, Queensland 4700, AUSTRALIA

²School of Engineering, James Cook University, Townsville, Queensland 4811, AUSTRALIA

ABSTRACT

A numerical model is presented for the single-phase fluid flow inside a sugar mill evaporator vessel. The model incorporates the effect of temperature and sugar concentration on the fluid properties. The model is a quarter wedge of the evaporator where the vertical heating tubes in the calandria section are modelled through a momentum source term in three directions. Although the use of the momentum source term in the calandria section did not result in fluid flow being completely restricted to the vertical direction, the predictions show reasonable agreement when compared with measurements taken from the actual vessel. The model presented here is capable of predicting trends in the fluid flow behaviour for processing conditions normally experienced in the final vessel of a multiple-effect evaporator set. The predictions show that the design of the juice distribution system at the inlet to the vessel has a major influence on the flow field in the remainder of the vessel. A large amount of mixing was found to occur at the inlet resulting in the calandria region being exposed to juice with properties close to the outlet stream, which is detrimental to performance.

NOMENCLATURE

A_o	open area ratio of tube-plate
B	sugar concentration by weight (%)
B_{fine}	sugar concentration for the fine mesh weight (%)
C_p	specific heat capacity (J/kg/K)
h_{fg}	latent heat of evaporation (J/kg)
\dot{m}_e	total average evaporation mass flow rate (kg/s)
\dot{m}_{evap}	modelled evaporation mass flow rate (kg/s)
\dot{m}_{in}	juice mass flow rate at vessel inlet (kg/s)
P	pressure (Pa)
Q_{tot}	total thermal energy into the system (W)
r	internal radius of the heating tube (m)
S_c	source term in continuity equation (kg/m ³ /s)
S_m	source term in momentum equation (kg/m ² /s ²)
S_e	source term in energy equation (J/m ³ /s)
T	fluid temperature (K)
T_{bpe}	boiling point elevation temperature (K)
T_{sat}	saturation temperature (K)
t	time (s)
u	velocity component in the x direction (m/s)
\mathbf{u}	velocity vector (m/s)
V	total velocity (m/s)
V_{fine}	total velocity for the fine mesh (m/s)
v	velocity component in the y direction (m/s)

w	velocity component in the z direction (m/s)
ΔV	difference in velocity at a node (m/s)
ΔB	difference in concentration at a node weight (%)
κ	thermal conductivity (W/m/K)
μ	dynamic viscosity (Pa.s)
ρ	density (kg/m ³)

INTRODUCTION

Multiple-effect evaporator vessels are used to boil off excess water contained in the juice of raw sugar, shown in Figure 1. The vessels, usually cylindrical in shape with conical bottoms, incorporate a bank of vertical heating tubes, known as a calandria. Heating steam condenses on the outside of the tube and juice boils within the tube. The vapour produced inside the tubes leaves the calandria and is used to heat the next vessel in the evaporator train. Little is known about the exact behaviour of fluid flow inside these vessels and calandria tubes, and the heat transfer process occurring within the heating tubes has not yet been examined closely.

Although there have been a number of papers dealing with heat transfer efficiency in evaporators (Watson 1986 & 1987), there is a dearth of work on their direct numerical simulation. Rouillard (1985) carried experimental studies of the convective boiling of sugar solutions and developed a one-dimensional model to predict mass flow and evaporation rates. Stephens and Harris (1999) modelled flow within a single tube in the calandria of a vacuum pan, using uni- and axisymmetric Eulerian two-phase flow models. They found that radial variations in temperature, velocity and volume fractions exist within a single tube. Steindl and Ingram (1999) presented some CFD modelling of an evaporator. The model was limited to the juice flow in the region below the calandria with a mass sink for water evaporation as a boundary condition accounting for the boiling in the calandria. The model showed that a recirculation region exists in the conical section of the evaporator, where fresh juice mixes with the evaporated juice descending from the calandria, reducing the thermal and concentration driving force for efficient evaporation in the calandria.

Stephens (2001) modelled a vacuum pan and demonstrated that modelling the flow in the calandria alone is extremely complex, due to the boiling phenomena. He adopted a segmented approach, rather than a comprehensive model, providing useful engineering solutions.

In this case, the evaporator could be segmented, with each segment either fully modelled by CFD or by a simplified model with boundary conditions linking the segments together. In the absence of data for the fluid flow in the heating tubes of the calandria, a model has been developed where the calandria has been simplified with a mass and heat balance model, which is then linked to a CFD model of the region below the calandria. This represents an important first step in modelling the evaporator. The model's ability to predict fluid flow is determined by comparing temperature and concentration predictions with measurements taken from the actual vessel.

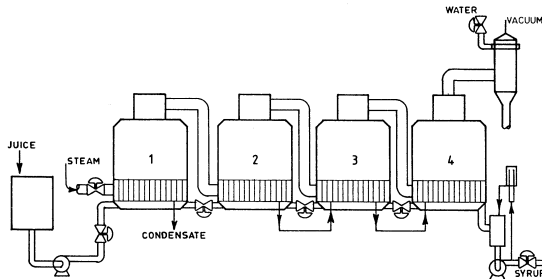


Figure 1: Multiple-effect evaporation in a four stage or set unit from Wright (1983).

THE EVAPORATOR

Juice supplied to the evaporator station contains 15wt% to 17wt% dissolved solids, with the rest being water, and exits the evaporator station at approximately 70wt%. Multiple-effect evaporation is achieved by connecting vessels in series (Figure 1), such that the first vessel is the only vessel supplied with low-pressure (LP) steam as the heating source. The vapour from the juice in the first vessel is used as the heating source for the second vessel, and so on down the evaporator set.

A temperature difference driving force is required to effect heat transfer and so the temperature of the vapour at the outlet of the vessel will always be lower than the LP steam or vapour supplied as the heating source. Cascading pressures inside the vessels along the set achieve this.

The evaporator vessel used for the basis of this study is the final vessel in a quadruple set, receiving juice at approximately 36 wt% solids to produce liquor at approximately 65 wt% solids. The vessel processes juice at a flow rate of approximately 250 to 270 t/hr at the inlet. This vessel was chosen for investigation because, as a final vessel, it has the largest change in dissolved solids concentration, of any vessel in the set.

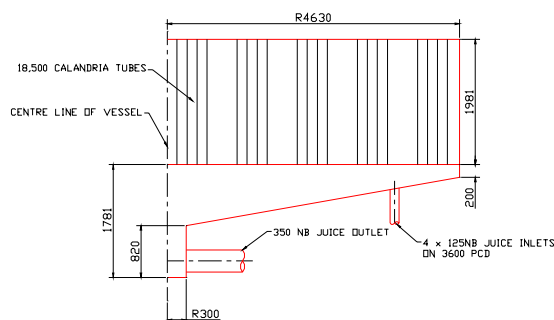


Figure 2: Side view of the vessel used for this study.

The diameter of the vessel is 9.26 m and the calandria is made up of 18553 tubes, each is 44.45-mm o.d. and 1.981 m in length. The calandria also has an array of 56 down-takes, each of 150 mm nominal bore (NB), distributed uniformly among the heating tubes. The total heating surface area of the vessel is 5265.7 m². Figure 2 shows the relevant dimensions important to this study.

Sugar juice is fed into the vessel via a four-point entry with a central juice outlet. At the inlet, an inverted L-shaped deflector plate (Figure 3) is placed over the vertical inlet pipe. The horizontal section of the plate completely covers the inlet pipe and the vertical section is on the side facing the centre of the vessel and runs to the floor of the vessel. The purpose of the plate is to divert incoming juice flow horizontally outwards, dissipating the jet formed by the inlet pipe. Experience has shown that without a deflector plate, or some other means of flow distribution, the jet from the inlet pipe severely erodes the bottom tube-plate.

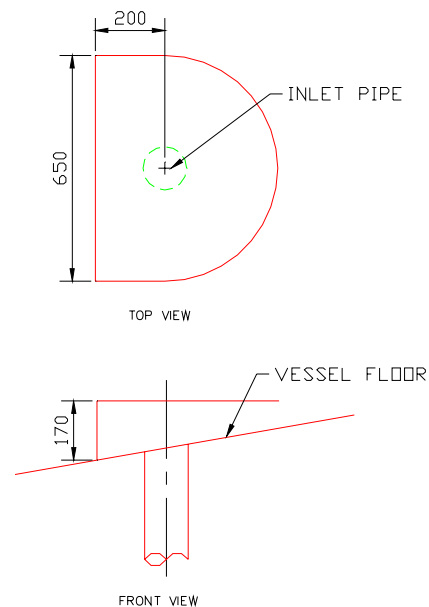


Figure 3: Details of the deflector plate used in the numerical simulations.

MODEL DESCRIPTION

Physical geometry

The vessel displays one-quarter symmetry, which was used to reduce the size of the computational mesh required. The regions above and below the calandria were modelled in detail with the conservation equations. The free surface in the region above the calandria was modelled with a rigid boundary with free slip. For simplicity, the effect of the calandria region was modelled as a pressure drop resulting from the flow of fluid through the heating tubes, through the laminar flow equations for frictional pipe flow. This pressure drop connected the regions above and below the calandria. It was assumed that the fluid flow was predominantly in the vertical direction due to the buoyancy generated by boiling within the tubes. To ensure that the vertical flow dominates, the pressure drop in the horizontal direction was set to a value much larger than

the maximum pressure drop in the vertical direction. In this work, the pressure drop in the two horizontal directions (x and z) were modelled as a momentum source, according to

$$\frac{dP}{dx} = -100.0u \quad (1)$$

$$\frac{dP}{dz} = -100.0w \quad (2)$$

The pressure drop in the vertical direction (y), assuming the fluid flow to be single phase and laminar, was approximated by

$$\frac{dP}{dy} = -\frac{8\mu}{r^2} \frac{|v|}{A_0} \quad (3)$$

The magnitude of the v velocity component is used since the flow is bi-directional. The A_0 term accounts for the tube area relative to the calandria section area. μ and v are the average viscosity and vertical velocity component respectively, obtained by averaging the inlet and outlet values.

From the first model run, dP/dy was found to be -1.7 Pa/m. This confirmed that the values chosen for dP/dx and dP/dz in equations (1) and (2) are large enough to ensure flow will be directed in the vertical direction at the boundary between the lower vessel and calandria base.

Heat flow

The total thermal energy, Q_{tot} , released by the condensing steam, neglecting thermal losses, was assumed to go into the latent heat of evaporation, producing vapour and sensible heating of the remaining liquid, due to the effect of boiling point elevation.

$$Q_{tot} = \dot{m}_e h_{fg} + \dot{m}_{in} C_p T_{bpe} \quad (4)$$

In equation 4, T_{bpe} is evaluated at the outlet and C_p is evaluated at the inlet.

As the simulation modelled the liquid phase, the energy converted to latent heat of the vapour formed during boiling was ignored, as it did not affect the simulation. Therefore, the heat source term was set to be equal to the sensible heating portion in equation 4. This assumption is valid so long as the evaporation rate, described in the next paragraph, is predicted correctly.

Evaporation

The conversion of the water in the juice to vapour was modelled by linking a mass sink term to the temperature of the fluid as follows:

$$\dot{m}_{evap} = \begin{cases} 0 & T < T_{sat} + T_{bpe} \\ \dot{m}_e & T \geq T_{sat} + T_{bpe} \end{cases} \quad (5)$$

The average evaporation is switched on or off if the fluid temperature is at, or below, the saturation temperature plus the boiling point elevation temperature.

Sugar concentration

The sugar concentration (B) was modelled as an additional variable in the transport equation and was allowed to be diffusive. The diffusivity coefficient was set to the average kinematic viscosity of the fluid at inlet and the outlet conditions. The convective transport dominates the diffusion of B .

Fluid properties

The fluid properties are functions of the fluid temperature (T) and the sugar concentration (B) and correlated through Equations 9 to 12, as listed in the Appendix.

Turbulence modelling

The standard $k-\varepsilon$ turbulence model was used for this investigation. Although some areas within the fluid flow are reasonably slow moving, and therefore possibly laminar, the turbulence model produced robust and stable simulations.

Single phase flow

The governing equations for incompressible single-phase flow with heat transfer are the unsteady Navier-Stokes equations in their conservation form.

The continuity (mass) equation is

$$\frac{\partial \rho}{\partial t} + \nabla \cdot (\rho \mathbf{u}) = S_c \quad (6)$$

The momentum equation is

$$\frac{\partial \rho \mathbf{u}}{\partial t} + \nabla \cdot (\rho \mathbf{u} \mathbf{u}) = -\nabla P + \mu \nabla^2 \mathbf{u} + \rho \mathbf{g} + S_m \quad (7)$$

The energy equation is

$$\frac{\partial \rho h}{\partial t} = -(\nabla \cdot \rho \mathbf{u} h) - (\nabla \cdot \mathbf{q}) + S_e \quad (8)$$

All of the equations detailed here were solved using CFX v5.5.1. The simulations were computed on a Pentium IV 2.4GHz processor with 2Gb of RAM, running Linux v7.3.

THE ACTUAL VESSEL

In order to provide validation of the model, plant measurements were made. The measurements included dissolved solids concentrations and temperatures at the inlet, outlet and at a number of locations in the juice space below the calandria. Measurements, required to provide boundary conditions for the model, were also taken.

Further details of the tests conducted are given in Pennisi (2002). Those data relevant to this study have been included in tabular form in the relevant section.

RESULTS AND DISCUSSION

Preliminary calculations

A simplified model, without heat flows and an evaporation rate limited to 10% of the actual plant performance, was used to test mesh size. Three mesh densities, coarse, medium and fine corresponding to 136219, 244773 and 594809 nodes respectively, were used.

The sugar concentration (B) and the velocity (V) were chosen as the variables for comparison purposes. It was found that the solution was still changing in moving from the coarse to the fine mesh. In all cases the location of the node where these values changed the most was near the inlet to the vessel, where velocity magnitudes are the highest. Differences in velocities were found to be largest at the boundaries, free surface and inlet sections of the model. As the mesh size is currently limited by the memory of the computer used, a final mesh containing

457653 nodes was chosen as a compromise and used for all remaining simulations. Furthermore, the mesh was redistributed to provide finer mesh points near the inlet region and coarser mesh points in regions where velocities and concentrations had small variations. Nevertheless, care must be exercised when examining predictions obtained from this model since it is likely that quantitative predictions may be in error and the magnitude of that error has yet to be determined.

Comparing predictions and measurements

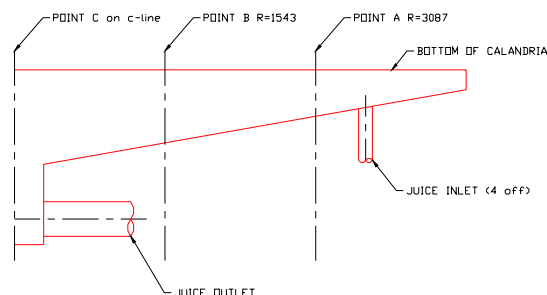


Figure 4: Location of the sample points on the actual vessel.

Measurements on the actual vessel were taken at the inlet, outlet and at three locations mid-way through the flow path as shown in Figure 4. The three sample points were located radially in a line from one of the inlets towards the central outlet. Point A is $\frac{2}{3}$ of the vessel radius away from the centre-line, Point B is $\frac{1}{3}$ of the vessel radius away from the centre-line and Point C is on the centre-line of the vessel.

Sampling tubes were inserted vertically through the bottom of the vessel for a range of distances below the bottom of the calandria. Table 1 shows the distances below the calandria for the four data sets used for this comparison, where positive values denote distances above the bottom tube-plate (*i.e.*, inside the heating tubes) and negative values denote distances below the bottom tube-plate.

Point	Vertical distance (m)			
	1	2	3	4
Test No.:	1	2	3	4
A	0.0	0.0	-0.2	-0.2
B	0.136	-0.064	-0.064	-0.264
C	-0.408	-0.608	-0.608	-0.808

Table 1: Sample point locations.

Due to natural fluctuations within the system, data points were logged for a 30-minute period to provide an average value. This period of logging also provided information on the extent of variation with time and the long-term performance of the evaporator. In general the concentration data varied within $\pm 4-5\%$ of the total concentration change from inlet to outlet and the temperature varied between $\pm 0.5^\circ\text{C}$.

Table 2 shows the results of all comparisons. The measured and predicted values are in good agreement, averaging a difference of only 1%. It also confirmed the flow in the bulk of the evaporator does not show steep

gradients in temperature or sugar concentration and can be modelled accurately with a coarse mesh.

	Temperature ($^\circ\text{C}$)		Concentration (% wt)	
	Measured	Predicted	Measured	Predicted
Test No. 1:				
A	55.1	56.2	63.5	63.0
B	55.0	56.2	65.0	63.0
C	57.0	56.2	63.6	62.9
outlet	55.2	56.2	63.1	62.9
Test No. 2:				
A	55.5	56.2	64.4	63.0
B	55.1	56.2	65.7	63.0
C	57.3	56.2	64.5	62.9
outlet	55.4	56.1	63.7	63.6
Test No. 3:				
A	55.5	58.2	68.5	67.4
B	55.1	58.2	72.9	67.4
C	57.3	58.2	67.1	67.4
outlet	55.4	58.2	67.5	67.4
Test No. 4:				
A	58.0	58.5	68.1	67.0
B	57.3	58.5	69.1	67.0
C	58.8	58.5	66.7	67.0
outlet	57.4	58.5	67.1	67.0

Table 2: Comparison of measured data against model predictions in the sugar evaporator.

The region around the inlet was found to have large velocity and concentration gradients. It is clear that the deflector plate plays an important role in defining the preliminary mixing within the evaporator.

Observation of fluid flow near the inlet

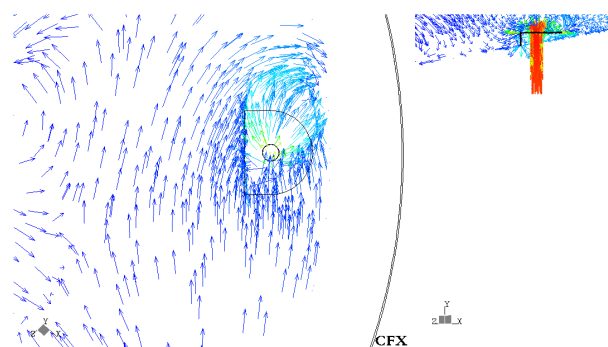


Figure 5: Vector plot of velocity field in a vertical plane through the inlet and a horizontal plane x mm from the top of the deflector plate.

Figure 5 shows the velocity field around the inlet. The juice enters the evaporator forming a jet. The deflector plate acts to spread the juice to prevent bypassing of the juice directly to the calandria tubes. As the deflector plate is directed to the outer diameter of the evaporator, the cross sectional area for flow reduces with distance. This causes the deflected inlet jet to accelerate. As it accelerates it also forms a vortex on flowing past the edge of the deflector. The vortex rolls up toward the calandria region with a juice stream flowing in the opposite direction below it. Two recirculation zones are set up around the jet

resulting in extensive mixing. The fluid flow through the outlet gives rise to a rotation in the evaporator. This rotation is constrained to a quarter slice model but in reality could produce a circular rotation to the whole evaporator. A full-scale numerical model should confirm this hypothesis and will be carried out in the future. This rotation is large enough to deflect the jet and promote the rapid mixing around the inlet.

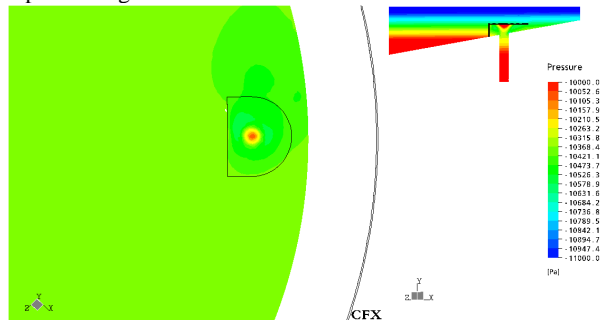


Figure 6: Pressure distribution contours in a vertical plane through the inlet and a horizontal plane 50 mm below the top of the deflector plate.

The recirculation zones that have been set up play an important part in the rapid mixing of the inlet and evaporator sugar solutions. The pressure contours in figure 6 show that hydrostatic pressure dominates over most of the evaporator, while at the inlet the stagnation pressure of the jet is the main source of acceleration for the fluid.

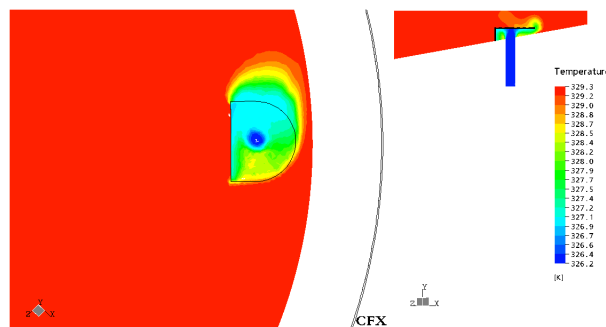


Figure 7: Temperature contours in a vertical plane through the inlet and a horizontal plane 50 mm below the top of the deflector plate.

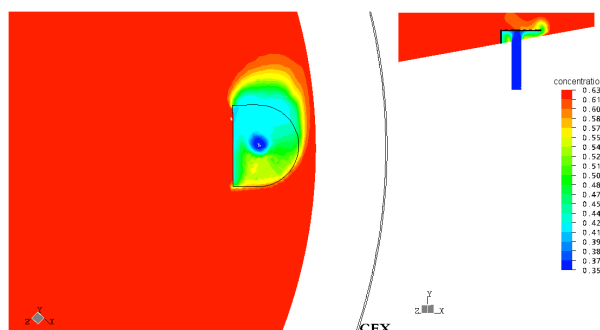


Figure 8: Sugar concentration contours in a vertical plane through the inlet and a horizontal plane 50 mm below the top of the deflector plate.

Figures 7 and 8 show the temperature and sugar concentration contours. The contours show that the temperature and sugar distribution are closely related, indicating that convective forces are responsible for the

rapid mixing of the inlet stream with the fluid in the evaporator. Hence, the calandria is essentially boiling a solution with only small changes in temperature/sugar concentration as it flows through the calandria tube.

Figures 7 and 8 also show that the temperature field is similar to the concentration field. This effect is expected as the boiling point elevation increases with sugar concentration and the magnitude of the thermal diffusivity is similar to the magnitude of the kinematic viscosity.

The results obtained have important implications. First, the experimental measurements of the temperature profile and sugar concentration in the region between the outlet and inlet deflector plate will show very small variations, probably too small to provide a means of validating the model. It would be necessary to measure the region around the inlet and the deflector plate to provide quality data for numerical validation. Second, the small change in the fluid properties in the bulk of the evaporator suggest that a simple model for boiling in the calandria should be attempted where temperature and sugar concentration changes are both minimal and the emphasis should be on the liquid/vapour fraction in the calandria region. Third, on a practical note, it appears from the measurements, as well as the predictions, that the majority of the juice below the calandria is at a concentration very close to that of the outlet. This is cause for concern in evaporator operation since the higher concentration material is harder to boil and therefore reduces the effectiveness of the installed heating surface area. Ideally the majority of the heating surface area should be exposed to the lowest concentration material.

The model also shows that the design of the juice inlet system, either deflector plate or otherwise, has a significant effect on the concentration and temperature distribution and hence, the boiling of the sugar solution. Although simplistic, this model provides designers with a means of testing various options to distribute the inlet flow for more effective introduction to the calandria tubes. The model also provides a starting platform for the development of more complicated and accurate models of the evaporator.

The current model has limited capability in handling the flow field inside the calandria region. The use of a fixed pressure gradient does not fully remove the existence of horizontal velocities, which is physically unrealistic. A more accurate and comprehensive model for the calandria for incorporation into the CFX model is an on-going project.

CONCLUSION

Three-dimensional numerical models of the liquid phase fluid flow inside the entire vessel geometry of a sugar mill evaporator have been presented. The model is capable of predicting trends for process conditions similar to those normally experienced in the final vessel of the set. There is a close link between the distribution of concentration and temperature due to the evaporation rate being arbitrarily set to the average value rather than being linked to the fluid properties.

An analysis of the fluid flow around the inlet has revealed that the design of the juice inlet and internal distribution system has a major effect on the overall vessel performance. The mixing action that is generated around the inlet to the vessel controls the concentration in the remainder of the vessel and causes large concentration and temperature gradients in the area adjacent to the inlet, with the remainder of the vessel being well mixed. The mixing action causes a majority of the heating tubes to be exposed to juice at a high sugar concentration that reduces effectiveness. This effect is less than ideal and is seen in the predictions and supported by the experimental data gathered from the actual vessel.

It should be noted that the model presented here is capable of predicting trends only and not absolute magnitudes. Future work on developing a more realistic representation of the vertical heating tubes should provide more accurate predictions of the flow in evaporators.

ACKNOWLEDGMENTS

The authors gratefully acknowledge the financial support provided by the Sugar Research Institute (SRI) and the Australian Research Council (ARC). The authors also acknowledge Proserpine Sugar Mill for allowing access to their evaporator set for monitoring.

REFERENCES

- INCROPERA, F. P. and DEWITT, D. P. (1996) "Fundamentals of heat and mass transfer", John Wiley & Sons, Brisbane, Queensland, Australia.
- PEACOCK, S. (1995), "Predicting physical properties of factory juices and syrups", *International Sugar Journal* 1995, Vol 97, No. 1162. John Roberts & Sons, Manchester, England.
- PENNISI, S. N. (2002), "Summary of evaporator test results – Proserpine Mill, #4 evaporator 2002 crushing season", SRI internal report 11/02, SRI, Mackay, Queensland, Australia.
- ROUILLARD, E.E.A (1985) "A study of boiling parameters under conditions of laminar non-Newtonian flow with particular reference to massecuite boiling", PhD thesis, University of Natal.
- STEINDL, R.J. and INGRAM, G.D. (1999), "Improved evaporator performance through circulation modelling", SRI syndicated project report 7/99, SRI, Mackay, Queensland, Australia.
- STEINDL, R.J. (1981), "Viscosity estimations for pan stage materials", Sugar Research Institute (SRI) technical circular 59, 1981. SRI, Mackay, Queensland, Australia.
- STEPHENS, D.W. (2001) "Modelling natural circulation in batch vacuum pans", PhD thesis, James Cook University.
- STEPHENS, D.W. and HARRIS, J. (1999) "Modelling convective boiling of molasses", 2nd International Conference on CFD in the Minerals and Processing Industries, CSIRO, Melbourne, Australia, 6-8 Dec, 393–398
- WATSON, L. J. (1986), "Heat transfer performance in evaporators Part 1. Theory and mechanisms", Sugar Research Institute (SRI) technical report 191. SRI, Mackay, Queensland, Australia.
- WATSON, L.J. (1987), "Heat transfer mechanisms in evaporators", Proc. Aust. Soc. of Sugar Cane Technologists, 221–227.

WRIGHT, P. G. (1983), "Juice heating and evaporation processes in the cane raw sugar industry", *CHEMECA '83, Proceedings of the 11th Australian conference on chemical engineering*, Brisbane, Queensland, Australia, 9–17.

APPENDIX A – CORRELATIONS USED

Density, Watson (1986b):

$$\rho = 1005.3 - 0.22556T - 2.4304 \times 10^{-3} T^2 + 3.7329B + 0.01781937B^2 \quad (9)$$

Viscosity, Steindl (1981):

$$\mu = 4.3 \times 10^{-4} \exp[3.357(B - 0.3155(T - 50)) / 116.8 - (B - 0.3155(T - 50))] \quad (10)$$

Thermal conductivity, Watson (1986):

$$\kappa = 0.574 + 1.699 \times 10^{-3} T - 3.608 \times 10^{-6} T^2 - 3.528 \times 10^{-3} B \quad (11)$$

Boiling point elevation, Peacock (1995):

$$T_{bpe} = 6.064 \times 10^{-5} \left(\frac{(273.15 + T)^2 B^2}{(374.3 - T)^{0.38}} \right) \times \left(5.84 \times 10^{-7} (B - 40)^2 + 7.2 \times 10^{-4} \right) \quad (12)$$